

1 Title:

2 **Isolation of chemically well-defined semipreparative liquid chromatography**  
3 **fractions from complex mixtures of proanthocyanidin oligomers and polymers**

4  
5 Authors:

6 Milla M. Leppä<sup>a</sup>, Maarit Karonen<sup>a</sup>, Petri Tähtinen<sup>a</sup>, Marica T. Engström<sup>a</sup>, Juha-Pekka Salminen<sup>a</sup>

7  
8 Affiliations:

9 <sup>a</sup>Natural Chemistry Research Group, Department of Chemistry, University of Turku,  
10 Vatselankatu 2, FI-20014 Turku, Finland

11  
12 Corresponding author contact information:

13 e-mail: [mimale@utu.fi](mailto:mimale@utu.fi)

14 mobile phone number: +358 29 450 3146

15 postal address: Vatselankatu 2, FI-20014 Turku, Finland

16  
17 Co-author contact information:

18 Maarit Karonen ([maarit.karonen@utu.fi](mailto:maarit.karonen@utu.fi))

19 Petri Tähtinen ([petri.tahtinen@utu.fi](mailto:petri.tahtinen@utu.fi))

20 Marica T. Engström ([mtengs@utu.fi](mailto:mtengs@utu.fi))

21 Juha-Pekka Salminen ([j-p.salminen@utu.fi](mailto:j-p.salminen@utu.fi))

22

23 Abstract:

24 In this study, a semipreparative liquid chromatography method was developed for the isolation of  
25 chemically well-defined proanthocyanidin (PA) oligomer and polymer fractions. The aim was to  
26 achieve better separation than traditionally achieved for the PAs with other chromatographic  
27 methods. The method was tested with eleven PA rich Sephadex LH-20 fractions, which originated  
28 from eleven different plant species. The resulting semipreparative fractions were analyzed by both  
29 triple quadrupole and high-resolution mass spectrometry assisted by ultrahigh-performance liquid  
30 chromatography (UPLC) separation. The results showed remarkable differences in the procyanidin  
31 to prodelphinidin ratio, mean degree of polymerization, and specific oligomeric and polymeric  
32 content. However, some of these features indicated consistent patterns between species as the  
33 function of UPLC retention time. The developed method enables the production of tens of well-  
34 defined fractions of PA oligomers and polymers from the unresolved chromatographic PA hump.  
35 Accordingly, this allows researchers to explore the most bioactive parts of the complex PA humps  
36 of any plant species, which have not been possible earlier.

37

38

39 Keywords:

40 Fractionation, HRMS, orbitrap, proanthocyanidin, semipreparative LC, UPLC-MS/MS

41

## 42 **1 Introduction**

43 Proanthocyanidins (PAs) are oligomers or polymers of flavan-3-ols (Fig. 1). The most common PA  
44 subunits are (epi)catechins with 3', 4'-dihydroxylation and (epi)gallocatechins with 3', 4', 5'-  
45 trihydroxylation in the B ring. As parts of the oligomeric or polymeric PA structures,  
46 (epi)catechins are called procyanidin (PC) units and (epi)gallocatechins as prodelphinidin (PD)  
47 units. These subunits are usually linked to each other via C<sub>4</sub>-C<sub>8</sub> or C<sub>4</sub>-C<sub>6</sub> bonds. PAs are abundant  
48 for example in legumes [1,2], which are used as animal feeds. In addition, a plant tissue may  
49 contain a diverse mixture of PA oligomers and polymers with varying PC/PD composition and  
50 degrees of polymerization [3].

51 Multiple positive bioactivities, such as antioxidant activity [4] and protein binding capacity  
52 [5], have been associated with PA-rich plants. It has been proposed, that PAs could play a major  
53 role in the ruminant-related bioactivities, such as antimethanogenic [6] and anthelmintic [7–11]  
54 activity. This has increased the interest towards PAs and their potential use as nutraceuticals [7,8],  
55 since nematodes of ruminants are not expected to build resistance towards plant PAs as rapidly as  
56 currently takes place with synthetic anthelmintic drugs [12,13]. If PAs could at the same time  
57 decrease methane emissions produced by enteric fermentation processes [14,15], then they could  
58 offer at least part of the solution to both, environmental [6] and parasitic [7–11,16] problems related  
59 to ruminant production.

60 The ruminant-related bioactivities of another tannin subgroup, hydrolysable tannins (HTs),  
61 have been studied during recent years by using pure HTs. For example, the different structural  
62 features of HTs have been linked to their *in vitro* anthelmintic activities [17]. Also, the degree of  
63 polymerization of HTs have been studied by the means of protein affinity [18] and  
64 antimethanogenic activity [19]. Such a detailed structural information is not available for PAs, since  
65 most of the bioactivity studies have been carried out with complex PA mixtures without the  
66 knowledge of defined structures of PAs. Thus the structure-bioactivity relationships are not fully

67 clear for PAs, but for instance the high content of PD subunits and the high mean degree of  
68 polymerization (mDP) have been associated with the high anthelmintic activity of PAs *e.g.* in the  
69 larval exsheathment inhibition assay [20,21]. To find out more detailed structure–bioactivity  
70 relationships for PAs, either pure compounds or chemically well-characterized mixtures of a few  
71 PAs, are needed.

72 A number of different chromatographic methods have been utilized in the PA isolation and  
73 purification, usually resulting in the purification of small oligomers (*e.g.* from dimers to pentamers)  
74 or mixtures of polymers. The further purification of the polymeric hump has been one of the main  
75 challenges. A common approach in PA fractionation is to use multistep elution with column  
76 chromatography, sometimes preceded by liquid-liquid extraction [22]. Liquid-liquid separation can  
77 be further exploited with chromatographic methods such as counter current chromatography (CCC)  
78 [23–25], and sequential centrifugal partition chromatography (SCPC) [26]. In these methods, two  
79 immiscible liquids are used as the mobile and stationary phases, thus ensuring the full recovery of  
80 the sample material during the fractionation. For instance, CCC has been used to isolate PA  
81 oligomers up to pentamers [23–25].

82 Different stationary phases and elution techniques have been utilized in column  
83 chromatography as well. For instance, Sephadex LH-20 and Toyopearl HW-50F are commonly  
84 used size exclusion chromatographic methods, which can produce large quantities of oligomeric  
85 and polymeric mixtures of PAs [27,28]. The Sephadex LH-20 chromatography can be carried out as  
86 traditional column chromatography, or the bed of the stationary phase can be placed *e.g.* in a  
87 Büchner funnel to achieve more rapid but less efficient purification [29]. For more accurate  
88 purification, even two-dimensional LC has been utilized [30,31]. Other LC techniques such as  
89 normal phase LC, has been used to separate PA oligomers up to hexamer [32] and semipreparative  
90 reversed-phase LC has been used to purify individual dimers [33]. However, we are unaware of  
91 chromatographic techniques that would be able to fractionate *e.g.* the polymeric PAs produced by

92 Sephadex LH-20 chromatography, into finer scale fractions containing only a small number of  
93 polymers, instead of the polymeric hump.

94 In this paper, we report a semipreparative liquid chromatography method that enables the  
95 controlled production of tens of chemically and chromatographically well-resolved PA fractions  
96 from the Sephadex LH-20 fractions rich in PA oligomers and polymers. The semipreparative  
97 method is accompanied by fraction analysis with UPLC-MS/MS [34] for the PC/PD ratio and mDP,  
98 and high-resolution mass spectrometry (HRMS) analysis for the accurate molecular masses of the  
99 PA oligomers and polymers. The method combination was tested with eleven model plant species  
100 to show that it was able to produce hundreds of chromatographically narrow PA fractions that  
101 varied in their retention time, PC/PD ratio and mDP. These methods provide tools to significantly  
102 improve our understanding of the complex nature of plant PAs and their bioactivities by large-scale  
103 production of different types of PA isolates followed by accurate structure–activity studies.

## 104 **2 Materials and methods**

### 105 **2.1 Solvents and materials**

106 Analytical grade acetone and methanol (VWR International S.A.S., France) were used in the  
107 extraction and Sephadex LH-20 column chromatography. Semipreparative LC analyses were carried  
108 out with HPLC grade acetonitrile (VWR International S.A.S., EC). Formic acid (99–100%, VWR  
109 Chemicals, EC) was used on eluent buffering. For the UPLC analyses LC-MS grade acetonitrile  
110 was purchased from VWR International S.A.S. (USA) and LC-MS grade formic acid from Sigma  
111 Aldrich. The water used was purified with Millipore Synergy UV (Merck KGaA, Darmstadt,  
112 Germany) system.

### 113 **2.2 Sample collection, extraction and Sephadex-LH 20 column chromatography**

114 Different types of tissues of eleven PA rich plant species were selected on the basis of their PA  
115 fingerprints to maximize the structural variability (PC/PD ratio, and mDP) of PAs used in this study  
116 (Table 1). The plant material was freshly collected into 1L glass bottles, which were then filled with

117 acetone. The samples were macerated in 4 °C for 9–12 months. After the maceration, the first  
118 extracts were separated from the plant material and plant tissues were ground. A new batch of  
119 extraction solvent (4/1 acetone/water, v/v) was added and the sample materials were dispersed with  
120 IKA disperser. Samples were further extracted 5–7 times with 4/1 acetone/water (v/v) until the  
121 extraction solvents were colorless. The acetone was evaporated from the solutions and the  
122 remaining aqueous extracts were freeze-dried.

123         Approximately 8–10 g of lyophilized extracts were dissolved in 40–50 mL of water. Water  
124 insoluble impurities were removed by centrifugation and filtration with 0.45 µm PTFE filters. The  
125 dissolved extracts were applied on top of a Sephadex LH-20 column (40 × 4.0 cm Chromaflex®,  
126 Kontes). Water phase was eluted and collected in two fractions (Sep1a: 1 × 150 mL, Sep1b: 1 × 350  
127 mL water), followed by two 500–600 mL methanol/water fractions (Sep2: 3/7 (v/v) MeOH/water,  
128 Sep3: 1/1 (v/v) MeOH/water) and three 500–600 mL acetone/water fractions (Sep4: 3/7 (v/v)  
129 Me<sub>2</sub>CO/water, Sep5: 1/1 (v/v) Me<sub>2</sub>CO/water, Sep6: 4/1 (v/v) Me<sub>2</sub>CO/water). Finally, the organic  
130 solvents were evaporated from the fractions by rotary evaporator and the aqueous fractions were  
131 lyophilized. The masses of the freeze-dried PA-rich Sephadex fractions of eleven plant species  
132 varied between 270–1630 mg.

### 133 **2.3 Semipreparative LC**

134 The semipreparative LC samples were prepared by dissolving 125–150 mg of isolated PA-rich Sep6  
135 fraction in 3 mL of water. Approximately five drops of ethanol were used to improve the  
136 dissolution before the addition of water. The samples were filtrated with 0.2 µm PTFE filters prior  
137 to the analysis. An HPLC system with a semipreparative column (150 × 21.20 mm, Gemini®  
138 10 µm, C-18, 110Å, Axia packed, Phenomenex) was used for further isolation of the studied PAs.  
139 The HPLC system consisted of a Waters 2535 Quaternary Gradient Module (Water Corp., USA), a  
140 Waters 2998 photodiode array Detector (Waters Corp., Singapore), and a Waters Fraction Collector  
141 III (Waters Corp., Japan). Acetonitrile (A) and 0.1% aqueous formic acid (B) were used as eluents.

142 For the elution, 12.0 mL min<sup>-1</sup> flow rate was used and fractions were collected into 2 ml tubes from  
143 5 to 33 min resulting in total of 168 individual fractions per one fractionation and each fraction  
144 containing the PAs eluting during 10 s retention time window. Before the elution, the column was  
145 thoroughly stabilized for 30 mins with 8% A in B. The elution was performed as follows: 0–4 min,  
146 isocratic 8% A in B; 4–32 min, 8–55% A in B (linear gradient); 32–35 min, 55–80% A in B (linear  
147 gradient), 35–80 min column wash and stabilization. From the retention time area, which inheld the  
148 complete PA fingerprint as detected by UV detection at 280 nm, every fourth fraction was selected  
149 and analyzed by UPLC-DAD-MS/MS and UPLC-DAD-HRMS.

150

#### 151 **2.4 UPLC-DAD-MS/MS analysis**

152 PC and PD units were detected with specific single reaction monitoring (SRM) methods for both  
153 extension and terminal units to allow the calculation of both PC and PD concentrations and mDP  
154 [34]. The detection of monomers, oligomers and polymers was enabled by the use of four different  
155 cone voltages in the fragmentation of the PC and PD units from the original PAs. Tandem mass  
156 analyses were performed with an Acquity UPLC system (Waters Corp., Milford, MA, USA) coupled  
157 to a Xevo TQ triple quadrupole mass spectrometer (Waters Corp., Milford, MA, USA). The UPLC  
158 system consisted of a sample manager, a binary solvent manager, a column, and a diode array  
159 detector. The column used was a Waters Acquity UPLC BEH Phenyl (1.7 μm, 2.1 × 100 mm  
160 Waters Corp. Wexferd, Ireland). For the elution, acetonitrile (A) and 0.1% aqueous formic acid (B)  
161 were used with 0.5 mL min<sup>-1</sup> flow rate. The elution profile was performed as follows: 0–0.5 min,  
162 0.1% A in B (isocratic); 0.5–5.0, 0.1–30% A in B (linear gradient); 5.0–8.0 min, 30–45% A in B  
163 (linear gradient); 8.0–11.5 min, column wash and stabilization. The data was recorded from 0 to 8  
164 min.

165 Negative ion mode was used in MS analyses, with electrospray ionization conditions  
166 described by Engström [34]. In short, the following values were used: capillary voltage 2.4 kV,

167 desolvation and source temperature 650 °C and 150 °C, respectively, desolvation and cone gas (N<sub>2</sub>)  
168 flow 100 and 1000 L h<sup>-1</sup>, respectively. The stability of ionization was monitored with 1 µg mL<sup>-1</sup>  
169 catechin solution (in acetonitrile/0.1% formic acid, v/v), which was analyzed five times before and  
170 after each batch of 10 samples [1]. The quantitation of PC and PD units and determination of mDP  
171 was performed as described by Engström et al. [34] and Malisch et al. [1]. The recorded PC and PD  
172 traces were smoothed (window size 5 scans × 2 smoothing iterations) with the Target Lynx  
173 software (V4.1 SCN876 SCN 917 © 2012 Waters Inc.) and converted into quantitative data by the  
174 help of calibration curves made separately for PC, PD and mDP. The PC and PD calibration curves  
175 were prepared by making dilutions in known concentrations (1.50–0.1875 mg mL<sup>-1</sup> for the PC  
176 standard and 2.00–0.25 mg mL<sup>-1</sup> for the PD standard) of two Sephadex LH-20 fractions with  
177 known PC and PD content that was initially calibrated against thiolysis results [34]. Calibration  
178 curves for the mDP were similarly obtained with six Sephadex LH-20 fractions with known PC and  
179 PD content and mDP.

## 180 **2.5 UPLC-DAD-HRMS analysis**

181 The analyses for accurate masses were carried out using an Aquity UPLC system (Waters Corp.,  
182 Milford, MA, USA) which was coupled to a quadrupole–Orbitrap mass spectrometer (Q  
183 Exactive™, Thermo Fisher Scientific GmbH, Bremen, Germany). The UPLC system was identical  
184 to the previously mentioned UPLC system, apart from the column, which in this case was an Aquity  
185 UPLC BEH Phenyl 1.7 µm, 2.1 × 30 mm column (Waters, Ireland). A flow rate of 0.65 mL min<sup>-1</sup>  
186 was utilized with the same solvents as described in the previous chapter. The elution profile was as  
187 follows: 0–0.1 min, 3% A in B (isocratic); 0.1–3.0 min, 3–45% A in B (linear gradient); 3.0–4.2  
188 min, column wash and stabilization. The UV ( $\lambda = 190–500$  nm) and MS data was detected  
189 throughout the analysis and analytes were detected as negative ions. A heated ESI source (H-ESI II,  
190 Thermo Fisher Scientific GmbH) was utilized with similar ionization source parameters as  
191 described by Suvanto *et al* [35]. In brief, the following parameters were used in the ionization

192 source: spray voltage,  $-3.0$  kV; capillary temperature,  $380$  °C; sheat, aux and sweep gas ( $N_2$ ) flow  
193 rate, 60, 20 and 0 arbitrary units respectively. In the orbitrap detector, the mass range was set at  
194  $m/z$  200–3000, the resolution was set at 70,000, and the automatic gain of  $3 \times 10^6$  was used.

195

### 196 **3 Results and discussion**

#### 197 **3.1 Sephadex LH-20 fractionation of eleven plant species**

198 Plant extracts were fractionated with Sephadex LH-20 column chromatography to produce  
199 PA-rich fractions. Since Sephadex LH-20 chromatography of tannins is largely based on their  
200 affinity to the gel rather than size exclusion, smaller PAs typically elute from the column before the  
201 large ones and the largest tannins are efficiently retained in the gel [36]. Thus, PAs eluted mainly in  
202 the two last fractions, Sep5 and Sep6. Sep5 fractions contained greater amount of other  
203 polyphenols, such as flavonoids (Supplementary material, Fig. 1) while Sep6 fractions contained  
204 mainly PA oligomers and polymers. Thus, Sep6 fractions were selected as the PA sources for the  
205 further purification by semipreparative HPLC. The UPLC-DAD chromatograms ( $\lambda = 280$  nm),  
206 PC/PD ratios and mDPs of the Sep6 fractions are displayed in supplementary material  
207 (Supplementary material, Fig. 2). Considerable variation was observed in the widths of the  
208 polymeric PA humps by UPLC-DAD. PAs of the most PD-rich fractions started to elute at the  
209 retention time of 2 min, while the PAs in the most PC-rich samples started to elute at 3 min or later.  
210 Since the PC-% and mDP varied between 2–99% and 4–20, respectively, these eleven fractions  
211 served together as a good source of PAs with respect to structural diversity for testing the efficiency  
212 of the semipreparative LC method.

#### 213 **3.2 Semipreparative LC fractionation of the Sep6 fractions**

214 Semipreparative LC fractionation of Sep6 fractions (Fig. 2) showed similar chromatographic  
215 profiles than was earlier obtained by UPLC. In semipreparative HPLC conditions, the elution of the  
216 PA humps started at 7–15 mins and lasted until at 22–30 mins, depending on the Sep6 fraction.

217 Every fourth semipreparative LC fraction (Sem fraction) was then analyzed by UPLC-DAD-  
218 MS/MS for their PC/PD ratio, mDP and UV chromatogram. Figure 3 shows the UV chromatograms  
219 ( $\lambda = 280$  nm) of *Lysimachia vulgaris* Sem fractions as an example to highlight how the  
220 semipreparative approach allowed the production of chromatographically defined PA fractions. In  
221 the UPLC analyses, the UV peak widths of Sem fractions varied between 0.3–1.2 min (Fig. 3) while  
222 the peak widths of original Sep6 fractions varied between 2.0–4.5 min (Supplementary Fig. 2). This  
223 clearly demonstrates the efficiency of the semipreparative LC fractionation in the separation of PAs.

224 In general, the isolated Sem fractions preserve their elution order (Fig. 3, Supplementary  
225 material Fig. 3A) when comparing the two chromatographic techniques. However, some  
226 irregularities were observed in the UPLC chromatograms of the Sem fractions. For instance, the  
227 latest Sem fractions produced wide UPLC peaks at earlier retention times than the previous  
228 fractions (Supplementary material Fig. 3B). This was interpreted to be due to the reversed-phase LC  
229 columns being unable to separate properly the largest PAs [37]. In addition, for instance Sem  
230 fractions 35, 39, 107 and 115 (Fig. 3), showed sharp UPLC peaks on the top of the more typical PA  
231 hump. These peaks were due to small PA oligomers or non-tannin impurities, especially flavonoids  
232 that elute simultaneously with the PA hump.

233

### 234 **3.3 UPLC-DAD-MS/MS results of the semipreparative LC fractions**

235 The UPLC-DAD-MS/MS [34] analyses revealed the PC and PD traces of the Sem fractions. Figure  
236 4 shows the PA fingerprints of 20 selected Sem fractions with different PC/PD ratios, mDPs and  
237 retention times. These examples revealed how the used fractionation method enabled the production  
238 of a highly diverse selection of different PA fractions ranging from almost PC pure to almost PD  
239 pure. For instance, the almost PC pure fractions (98–99% PC), which eluted from 3.5 to 6 minutes  
240 (Fig. 4A–D), were different either by their mDP (4–17) or retention time. Thus, they were all  
241 chemically different. For example, *Aesculus hippocastanum* Sem fraction 116 (Fig. 4C) and

242 *Trifolium medium* Sem fraction 82 (Fig. 4B) had similar PC/PD ratios and mDP, but they still  
243 eluted at different retention times. One explanation for this may lay in the composition of PA  
244 oligomers and polymers. *A. hippocastanum* Sem fractions (Fig. 4C) were rich in A-type PAs whilst  
245 only B-type PAs were found in the *T. medium* Sem fractions (Fig. 4B). Similar variability was  
246 observed with different PC/PD mixtures (Fig. 4E–R) and almost pure PDs (Fig. 4S–T). For  
247 instance, *Lotus corniculatus* Sem fraction 92 (Fig. 4J) and *Pinus sylvestris* Sem fraction 78  
248 (Fig. 4K) had almost similar mDPs and PC/PD ratios, but they differed from each other by retention  
249 times which were 4.5 and 4.0 min respectively.

250 Altogether, hundreds of fractions were obtained with either different PC/PD ratios, mDPs  
251 and/or retention times. The retention time of the fraction as such did not reveal much of their  
252 chemical composition. A fraction eluting at 4 mins could be either 99% PC with the mDP of 4 (Fig.  
253 4A), 60% PC with the mDP of 18 (Fig. 4I), or 30% PC with the mDP of 30 (Fig. 4P). Such a  
254 diversity of PA chemistry within the hundreds of fractions, enables the more accurate determination  
255 of structure–activity relationships of PAs. The above-mentioned data of the hundreds of  
256 semipreparative fractions were used to create species-specific elution profiles of PC/PD ratios and  
257 mDPs.

### 258 **3.4 Distribution of PCs, PDs and mDP in semipreparative LC elution**

259 The distribution of PC and PD units during the semipreparative LC analysis varied significantly  
260 among different samples. To make the conclusions more uniform, the samples were categorized  
261 into five groups depending on their total PC/PD ratio **I**: PC-%  $\geq$  98%; **II**: PC-% = 97–61%; **III**: PC-  
262 % = 60–41 %; **IV**: PC-% = 40–21%; **V**: PC-%  $\leq$  20% (group III included only one sample,  
263 therefore the figure is displayed in supplementary material only, Supplementary Fig.4).

264 Group **I** included Sep6 fractions of *Trifolium medium* and *Aesculus hippocastanum*. In the  
265 group **I**, the PC content was constant at 99% (Fig. 5A) for almost throughout the analysis. Only the  
266 first four analyzed fractions from the retention time of 12–15 mins contained 1–17% PD units. In

267 total, the mDP increased during the elution, but with *A. hippocastanum* (supplementary data Fig. 4)  
268 the mDP decreased slightly in at certain retention time points. The decreases appear at the same  
269 retention times as single peaks in the semipreparative UV chromatogram ( $\lambda = 280$  nm). Thus, the  
270 early eluting smaller oligomers temporarily distorted the mDP curve.

271 Group **II** included *Larix sp.*, *Rhododendron schlippenbachii* Maxim. and *Rhododendron*  
272 *dichroanthum* Diels. In group **II** (Fig. 5B and supplementary Fig. 4), an interesting pattern in  
273 PC/PD ratio was discovered. When the PAs started to elute, the first eluting compounds were PD-  
274 rich oligomers. However, at the retention time of 13.2–15.4 min, the most abundant subunit type  
275 changed from PD to PC, after which, the PC content was settled between 60–90%. Apart from the  
276 other groups, the mDP did not increase continuously during elution in group **II**.

277 Group **III** contained one sample, the Sep6 fraction of *Lotus corniculatus* (Supplementary  
278 Fig. 4). Nevertheless, a characteristic feature for this sample was that, the mDP increased during the  
279 elution and the PC/PD ratio settled close to 50/50 after 15.6 min retention time. The results  
280 indicated that the main compounds in the *L. corniculatus* were PAs consisting of both subunits, PC  
281 and PD rather than PC or PD pure oligomers.

282 Group **IV** included the Sep6 fractions of *Lysimachia vulgaris* and *Pinus sylvestris*. In the **IV**  
283 group, the mDP increased relatively steadily throughout the elution while the PC/PD ratio varied  
284 greatly. For example the PD content of the *L. vulgaris* (Fig. 5C) sample, varied between 97–31%  
285 during the elution. An interesting pattern of PC/PD ratio was observed with *Pinus sylvestris*  
286 fractions as well (Supplementary Fig. 5). At the beginning of the elution, the PD content was  
287 > 80%, after which it decreased to 55%. But after the retention time of 16.5–18.6 min, the amount  
288 of PD units increased again up to 73%. PD units are considered more hydrophilic than the PC units,  
289 thus according to a general assumption, the PD-rich PAs should elute prior to the PC-rich ones.  
290 This data however indicated that the PD content could increase during the elution. Also, the mDP  
291 increased during the elution. Hence, the late eluting polymers had two structural features, which

292 affect the retention, the early elution due to additional -OH groups and the late elution due to the  
293 large polymer size [1].

294 The last group included the Sep6 fractions of *Salix phylicifolia*, *Ribes alpinum* and *Trifolium*  
295 *repens*. In the group V (Fig. 5D, Supplementary Fig. 5), the mDP shows an unusual pattern. In  
296 general, the mDP increased during the elution, but at 3–5 min after the most intensive point at  
297 semipreparative chromatogram ( $\lambda = 280$  nm), the mDP reached a local maximum, after which the  
298 mDP decreased again. This indicates that the largest oligomeric and polymeric PAs in PD-rich  
299 samples eluted 3–5 min after the most abundant and slightly smaller PAs. PDs remained as the most  
300 abundant subunit type throughout the analysis in the group V.

301 Even though the samples were diverse in their PC/PD ratios and mDP distributions, some  
302 characteristic features were common for all analyzed samples. For example, the PD-% values were  
303 highest at the beginning of the elution in all five groups. The increased hydrophilicity of the PD rich  
304 oligomers was the most likely cause of the early elution. In addition, the changes of mDP during  
305 the elution were variable between different PA composition groups. The most usual trend of the  
306 mDP was, that it increased by retention time. The increase was most considerable in PC (group I)  
307 and PD (group V) rich groups whilst in the group II the changes in mDP did not seem to have a  
308 systematic pattern. It seemed that, when the used Sep6 fractions were either PC or PD rich, the  
309 mDP increased steadily during the elution. In these cases, the main factor affecting the retention  
310 was the size of the oligomers, thus the largest oligomers eluted later.

311 Altogether, the PA mixtures included a great variety of different mDPs and subunit  
312 compositions. For example, the Sep6 fraction of *Larix sp.* (Fig. 5B) had the average PC/PD ratio of  
313 62/38 whereas the most PD-rich fraction from semipreparative LC analysis contained 97% PDs and  
314 the most PC-rich fraction contained only 11% PDs. Only few fractions had the average PC/PD ratio  
315 of approximately 60/40 and generally, the composition of the produced semipreparative LC  
316 fractions differed significantly from the average composition of the Sep6 fractions. Thus, it is

317 possible to isolate a large variety of different PA mixtures from a single pre-purified plant sample  
318 with the semipreparative LC elution protocol introduced in this paper.

### 319 **3.5 UPLC-DAD-HRMS results of the semipreparative LC fractions**

320 All semipreparative fractions that were analyzed by quantitative MS/MS were analyzed also by  
321 high-resolution mass spectrometry (HRMS) with an UPLC-Q-Orbitrap-MS instrument. PAs are  
322 prone to fragmentation [38,39] thus the possibility of detecting quinone-methide fragments as  
323 molecular or multiply charged ions was taken into account at the early stage of the mass spectral  
324 interpretation. Figure 6 displays the retention time shifts of multiple extracted ion chromatograms  
325 (EICs) of PC-rich PAs in *Lysimachia vulgaris* Sem fraction 91. The chromatographic humps of PAs  
326 shifted to latter retention times when the DP (degree of polymerization) of oligomers and polymers  
327 increased. EICs overlapped, but since they were not identical, they probably originated from  
328 different compounds. Thus, the most significant peaks in the forecoming high-resolution mass  
329 spectra, were interpreted as molecular  $[M-H]^-$  or multiply charged ions  $[M-XH]^{X-}$  instead of  
330 fragments. Herein, the observations from high-resolution mass data are described through four  
331 representative semipreparative LC fractions of *Lysimachia vulgaris* and *Larix sp.*

332 Large proanthocyanidins tend to form multiply charged ions in the electrospray ionization  
333 source [40]. Depending on the degree of polymerization, the PAs formed doubly (DP 4–11, Fig. 7  
334 and 9), and triply charged ions (DP 10–20, Fig. 7 and 8). Even four-fold charged ions were  
335 observed (DP > 18) in the *L. vulgaris* Sem fraction 91 (Fig. 8). Due to the multiply charged ions,  
336 certain patterns were observed in the mass spectra. In the case of PC-rich samples, the PC pure  
337 oligomers and polymers were observed as at  $m/z$   $577.13 + 288.06n$  for singly [37,41], at  $m/z$   $576.13$   
338  $+ 144.03n$  for doubly and at  $m/z$   $959.87 + 96.02n$  for triply charged ions (Fig. 8). In the case of PD-  
339 rich samples the PA oligomers and polymers were observed as at  $m/z$   $609.12 + 304.06n$  for singly,  
340 at  $m/z$   $608.12 + 152.03n$  for doubly and at  $m/z$   $1013.19 + 101.35n$  for triply charged ions. The  
341 smallest observed oligomers for each charge state were dimers ( $z = 1-$ ), tetramers ( $z = 2-$ ) and

342 decamers ( $z = 3-$ ). The number of additional PC or PD units is described with  $n$ , where  $n \geq 0$  is the  
343 amount of additional PC or PD unit to the smallest oligomers.

344 Systematic oligomer series were observed within each polymer size as well. Within a single  
345 oligomer size, an increment of  $m/z +16.00$  for singly,  $+8.00$  for doubly,  $+5.33$  for triply and  $+4.00$   
346 for fourfold charged ions was observed. These systematic increases in the mass spectra were caused  
347 by a difference of one subunit being PD instead of PC. For instance, *L. vulgaris* Sem fraction 67  
348 contained a doubly charged PC pure heptamer at  $m/z$  1008.22 and a doubly charged PC rich  
349 heptamer consisting of  $6 \times \text{PC} + 1 \times \text{PD}$  unit at  $m/z$  1016.22 (Fig. 7C–D and 8C). Thus, their  $m/z$   
350 difference was 8.00.

351 The differences between *L. vulgaris* Sem fraction 67 (Fig. 7) and 91 (Fig. 8) demonstrated the  
352 changes of PA oligomer composition in different retention time points of the semipreparative  
353 elution. The Sem fraction 67 of *L. vulgaris* included a mixture of oligomers ranging from PC pure  
354 to PD pure (Fig. 7, Table 2) and the degree of polymerization ranged between 4–17 subunits.  
355 Within at  $m/z$  range of 960–1120 (Fig. 7B), three oligomeric and polymeric PA series were  
356 observed. These were doubly charged series of heptameric (DP 7) and triply charged series of  
357 decameric (DP 10) and undecameric (DP 11) PAs. In the case of heptameric oligomer series (Fig.  
358 7C), the PC pure oligomer (at  $m/z$  1008.2207, Table 2) was observed as the most intensive  
359 oligomer. The oligomeric composition of heptamer ranged from  $7 \times \text{PC} + 0 \times \text{PD}$  units (at  
360  $m/z$  1008.2207) to  $1 \times \text{PC} + 6 \times \text{PD}$  units (at  $m/z$  1056.2028). The  $m/z$  addition to the previous  
361 signal was 8.00 Da and all PC/PD combinations were found except for PD pure heptamer. In the  
362 undecameric PA series (Fig. 7D), the most abundant oligomer consisted of  $3 \times \text{PC} + 8 \times \text{PD}$  units  
363 (at  $m/z$  1098.5461, Table 2). The undecameric oligomer series ranged from  $10 \times \text{PC} + 1 \times \text{PD}$  units  
364 (at  $m/z$  1061.2260) to  $1 \times \text{PC} + 10 \times \text{PD}$  units (at  $m/z$  1109.2085). The  $m/z$  addition to the previous  
365 signal was 5.33 Da, when the oligomers differed from each other by one subunit. Similar  
366 distribution patterns of PC and PD units were observed with other oligomer sizes as well, thus

367 indicating that the *L. vulgaris* Sem fraction 67 was a diverse mixture of oligomeric and polymeric  
368 PAs containing both PC and PD subunits.

369 Sem fraction 91 of *L. vulgaris* consisted mainly of PC-rich oligomers (Fig. 8A, Table 3) and  
370 the most intensive ions in the mass spectrum were PC pure oligomers. The polymerization of the  
371 compounds ranged between 5–25 subunits. The closer examination of the spectrum revealed the  
372 composition of subunits in more detail. For example at the  $m/z$  range of 1510–1560 (Fig. 8B),  
373 polymers consisting of 16 ( $z = 3^-$ ) and 21 ( $z = 4^-$ ) subunits were observed. The most intensive  
374 compounds in both PA series were PC-pure polymers. In the fourfold charged 21-meric PA series,  
375 the polymers ranged from  $21 \times \text{PC} + 0 \times \text{PD}$  (at  $m/z$  1511.8209, Fig. 8C, Table 3) to  
376  $17 \times \text{PC} + 4 \times \text{PD}$  units (at  $m/z$  1527.8123). In the hexadecameric series of PAs, the polymers  
377 ranged from  $16 \times \text{PC} + 0 \times \text{PD}$  (at  $m/z$  1535.9923, Table 3) to  $14 \times \text{PC} + 2 \times \text{PD}$  units (at  $m/z$   
378 1546.6559). In the polymeric series of the fourfold charged ions, the addition of 4.00 Da was  
379 observed to the previous signal, when the PC/PD subunit content increased by one PD unit.

380 The high-resolution mass spectra showed significantly differing PA compositions in *L.*  
381 *vulgaris* Sem fractions 67 and 91. The qualitative differences between the high-resolution mass  
382 spectra, were similar to the differences observed in the qualitative MS/MS data. Larger polymers  
383 were identified in the Sem fraction 91 (mDP = 27) than in the Sem fraction 67 (mDP = 23). Also,  
384 Sem fraction 91 (PC/PD = 68/32) was distinctively PC-rich whereas Sem fraction 67  
385 (PC/PD = 36/64) consisted of both PC and PD-rich oligomers and polymers. The difference in the  
386 ionization efficiency of PC and PD units is the most probable reason why Sem fraction 91 seemed  
387 to contain such PC pure composition whilst Sem fraction 67 consisted of a large variety of PC and  
388 PD containing oligomers. PC-rich oligomers are more easily ionized, and therefore, their relative  
389 abundance in the mass spectra might seem excessive. Nevertheless, the diversity of the PA  
390 oligomers and polymers was more significant with Sem fraction 67 than in Sem fraction 91. This

391 was observed especially from the numbers of different PC/PD unit combinations in each oligomeric  
392 or polymeric PA series.

393 Another representative example of the differences which emerge during the semipreparative  
394 LC, were observed in *Larix sp.* Sem fractions 74 and 94 (Fig. 9). Both of these samples were PC-  
395 rich and the most intensive signals of the oligomers were PC pure oligomers. The most considerable  
396 differences between the mass spectra of fractions 74 and 94 were found in the relative intensity of  
397 individual oligomers and their polymeric size. The largest polymer in *Larix sp.* Sem fraction 74 was  
398  $14 \times$  PC (Fig. 9A), and in Sem fraction 94 it was  $20 \times$  PC (Fig. 9B). In the fraction 74, the most  
399 abundant PA oligomers ranged from dimer to hexamer, whereas the fraction 94 included a variety  
400 of oligomers with relative abundance of  $> 40 \%$ , ranging from 6 to 13 subunits. These differences in  
401 high-resolution mass spectra were similar to the differences observed in the mDP measured by  
402 tandem MS. The fraction 74 contained a less complex composition of PAs and the most abundant  
403 oligomers were smaller than in the fraction 94. The mDPs of the above-mentioned fractions were  
404 8.4 and 13.3 respectively.

405 The separated fractions were highly complex in PA composition, thus, the original mixtures  
406 of PA oligomers and polymers must have been even more complex. The fractionation of PA  
407 oligomers enabled the detailed identification of PAs by high-resolution mass spectra. By  
408 fractionation, even the PAs in minor concentrations were accumulated and identified. These  
409 findings show that the average PC/PD or mDP values of the PA mixtures produced by e.g.  
410 Sephadex LH-20 gel chromatography, did not give a rightful impression of the individual  
411 compounds in the samples. Instead, individual PA isolates produced from the Sephadex LH-20  
412 fractions, may possess such different composition of oligomers and polymers that cannot be  
413 estimated from the mDP or average PC/PD ratio of the original plant sample or Sephadex LH-20  
414 fraction.

415

## 416 **4 Conclusions**

417 In present study, we developed a semipreparative LC method, which can be exploited in the  
418 fractionation of pre-purified PAs into tens of different PA fractions. The retention time windows of  
419 the fractionated PAs were significantly narrower than the retention time windows of the original PA  
420 samples. The semipreparative fractions also preserved their elution order in the UPLC conditions.  
421 The closer investigation of the semipreparative PA fractions revealed a great variability in PC/PD  
422 compositions, mDPs and retention times. Semipreparative elution profiles of the PC/PD ratios and  
423 mDPs were presented along with the semipreparative LC chromatograms ( $\lambda = 280$  nm). The elution  
424 patterns of PC and PD units and mDPs were rather species specific and highly dependent on the PA  
425 composition of the Sephadex-LH 20 fractions. The main conclusions regarding the semipreparative  
426 elution were the early elution of PD rich PAs compared to the PC rich ones, and the elution of  
427 smaller oligomers prior to larger ones in the case of either PC or PD rich sample. Altogether, major  
428 changes in PC/PD ratios emerged during semipreparative elution, thus indicating high versatility of  
429 PA molecules in the Sephadex-LH 20 fractions.

430 Individual PAs were identified with high-resolution mass spectrometry. The identification of  
431 compounds confirmed the quantitative MS/MS measurements and revealed the PC/PD variability  
432 within single fractions. Even fractions purified from the very same plant source, were divergent in  
433 their subunit composition and polymer size. This study elaborates our understanding about the PA  
434 composition beneath the previously unresolved chromatographic hump and provides tools for the  
435 production of tens and hundreds of PA isolates with known chemical composition.

## 436 **5 Appendix 1**

437 DAD, diode array detector; DP, degree of polymerization; mDP, mean degree of polymerization;  
438 PA, proanthocyanidin; PC, procyanidin; PC/PD, the ratio of procyanidin and prodelfphinidin units;  
439 PD, prodelfphinidin; QqQ, triple quadrupole; Sep5; Sephadex LH-20 fraction 5, Sep6, Sephadex

440 LH-20 fraction 6; SRM, single reaction monitoring; UPLC, ultrahigh-performance liquid  
441 chromatography.

442

## 443 **6 Acknowledgements**

444 We thank Anne Koivuniemi for the maintenance of the analysis equipment and Suvi Vanhakylä for  
445 the collection of the plant material. The crew of Natural Chemistry Research Group is  
446 acknowledged for all the general help in the laboratory.

447

## 448 **7 Funding Sources**

449 We acknowledge Raisio Research Foundation and Academy of Finland (298177) for the funding of  
450 this research. A purchase of the UHPLC-DAD-QqQ system was made possible by a Strategic  
451 Research Grant of the University of Turku (Ecological Interactions).

452

## 453 **8 Supplementary Material Description**

454 Figure 1. UPLC-DAD UV traces ( $\lambda = 280$  nm) of Sephadex LH-20 fractionation of *Larix sp.*

455 Figure 2. UPLC-DAD UV traces ( $\lambda = 280$  nm) of Sep6 fractions of the eleven plant species.

456 The abbreviations are as follows: Sep6 fraction, the 6<sup>th</sup> Sephadex LH-20 fraction eluted with  
457 4/1 (v/v) acetone water; mDP, mean degree of polymerization; PC/PD, ratio of procyanidin  
458 and prodelphinidin units.

459 Figure 3. UPLC-DAD UV traces ( $\lambda = 280$  nm) of semipreparative LC fractionation of *Ribes*  
460 *alpinum* and *Trifolium medium*.

461 Figure 4. Semipreparative LC DAD traces ( $\lambda = 280$  nm) with mDP and PC/PD distribution  
462 of *Aesculus hippocastanum*, *Rhododendron dichroanthum*, *Rhododendron schlippenbachii*  
463 and *Lotus corniculatus*.

464 Figure 5. Semipreparative LC DAD traces ( $\lambda = 280$  nm) with mDP and PC/PD distribution  
465 of *Pinus sylvestris*, *Salix phylicifolia* and *Trifolium repens*.

466

## 467 9 References

- 468 [1] C.S. Malisch, A. Lüscher, N. Baert, M.T. Engström, B. Studer, C. Fryganas, D. Suter, I.  
469 Mueller-Harvey, J.P. Salminen, Large Variability of Proanthocyanidin Content and  
470 Composition in Sainfoin (*Onobrychis viciifolia*), *J. Agric. Food Chem.* 63 (2015) 10234–  
471 10242. doi:10.1021/acs.jafc.5b04946.
- 472 [2] J.H. Niezen, T.S. Waghorn, W.A.G. Charleston, G.C. Waghorn, Growth and gastrointestinal  
473 nematode parasitism in lambs grazing either lucerne (*Medicago sativa*) or sulla (*Hedysarum*  
474 *coronarium*) which contains condensed tannins, *J. Agric. Sci.* 125 (1995) 281.  
475 doi:10.1017/S0021859600084422.
- 476 [3] I. Mueller-Harvey, G. Bee, F. Dohme-Meier, H. Hoste, M. Karonen, R. Kölliker, A. Luscher,  
477 V. Nidekorn, W.F. Pellikaan, J.-P. Salminen, L. Skot, L.M.J. Smith, S.M. Thamsborg, P.  
478 Totterdell, I. Wilkison, A.R. Williams, B.N. Azuhnwi, N. Baert, A.G. Brinkhaus, G. Copani,  
479 O. Desrues, M.T. Engström, C. Fryganas, M. Girard, N.T. Huyen, K. Kempf, C. Malisch, M.  
480 Mora-Ortiz, J. Quijada, A. Ramsay, H.M. Ropiak, G.C. Waghorn, Benefits of Condensed  
481 Tannins in Forage Legumes Fed to Ruminants: Importance of Structure, Concentration and  
482 Diet Composition, *Crop Sci.* (2017). doi:10.2135/cropsci2017.06.0369.
- 483 [4] Y. Gong, F. Fang, X. Zhang, B. Liu, H. Luo, Z. Li, B Type and Complex A/B Type  
484 Epicatechin Trimers Isolated from *Litchi pericarp* Aqueous Extract Show High Antioxidant  
485 and Anticancer Activity, *Int. J. Mol. Sci.* 19 (2018) doi:10.3390/ijms19010301.
- 486 [5] W.E. Zeller, M.L. Sullivan, I. Mueller-Harvey, J.H. Grabber, A. Ramsay, C. Drake, R.H.  
487 Brown, Protein precipitation behavior of condensed tannins from *Lotus pedunculatus* and  
488 *Trifolium repens* with different mean degrees of polymerization, *J. Agric. Food Chem.* 63

- 489 (2015) 1160–1168. doi:10.1021/jf504715p.
- 490 [6] B. Hatew, E. Stringano, I. Mueller-Harvey, W.H. Hendriks, C.H. Carbonero, L.M.J. Smith,  
491 W.F. Pellikaan, Impact of variation in structure of condensed tannins from sainfoin  
492 (*Onobrychis viciifolia*) on *in vitro* ruminal methane production and fermentation  
493 characteristics, J. Anim. Physiol. Anim. Nutr. (Berl). 100 (2016) 348–360.  
494 doi:10.1111/jpn.12336.
- 495 [7] H. Hoste, J.F.J. Torres-Acosta, C.A. Sandoval-Castro, I. Mueller-Harvey, S. Sotiraki, H.  
496 Louvandini, S.M. Thamsborg, T.H. Terrill, Tannin containing legumes as a model for  
497 nutraceuticals against digestive parasites in livestock, Vet. Parasitol. 212 (2015) 5–17.  
498 doi:10.1016/j.vetpar.2015.06.026.
- 499 [8] H. Hoste, F. Jackson, S. Athanasiadou, S.M. Thamsborg, S.O. Hoskin, The effects of tannin-  
500 rich plants on parasitic nematodes in ruminants, Trends Parasitol. 22 (2006) 253–261.  
501 doi:10.1016/j.pt.2006.04.004.
- 502 [9] J. Quijada, C. Fryganas, H.M. Ropiak, A. Ramsay, I. Mueller-Harvey, H. Hoste,  
503 Anthelmintic Activities against *Haemonchus contortus* or *Trichostrongylus colubriformis*  
504 from Small Ruminants Are Influenced by Structural Features of Condensed Tannins, J.  
505 Agric. Food Chem. 63 (2015) 6346–6354. doi:10.1021/acs.jafc.5b00831.
- 506 [10] A.L. Molan, Effect of purified condensed tannins from pine bark on larval motility, egg  
507 hatching and larval development of *Teladorsagia circumcincta* and *Trichostrongylus*  
508 *colubriformis* (Nematoda: Trichostrongylidae), Folia Parasitol. (Praha). 61 (2014) 371–376.  
509 doi:10.14411/fp.2014.036.
- 510 [11] A.R. Williams, H.M. Ropiak, C. Fryganas, O. Desrues, I. Mueller-Harvey, S.M. Thamsborg,  
511 Assessment of the anthelmintic activity of medicinal plant extracts and purified condensed  
512 tannins against free-living and parasitic stages of *Oesophagostomum dentatum*, Parasit.  
513 Vectors. 7 (2014) 518. doi:10.1186/s13071-014-0518-2.

- 514 [12] R.M. Kaplan, Drug resistance in nematodes of veterinary importance: A status report, Trends  
515 Parasitol. 20 (2004) 477–481. doi:10.1016/j.pt.2004.08.001.
- 516 [13] J.F.J. Torres-Acosta, P. Mendoza-de-Gives, A.J. Aguilar-Caballero, J.A. Cuellar-Ordaz,  
517 Anthelmintic resistance in sheep farms: update of the situation in the American continent,  
518 Vet. Parasitol. 189 (2012) 89–96. doi:10.1016/j.vetpar.2012.03.037.
- 519 [14] J.A. Foley, N. Ramankutty, K.A. Brauman, E.S. Cassidy, J.S. Gerber, M. Johnston, N.D.  
520 Mueller, C. O’Connell, D.K. Ray, P.C. West, C. Balzer, E.M. Bennett, S.R. Carpenter, J.  
521 Hill, C. Monfreda, S. Polasky, J. Rockström, J. Sheehan, S. Siebert, D. Tilman, D.P.M. Zaks,  
522 Solutions for a cultivated planet, Nature. 478 (2011) 337–342. doi:10.1038/nature10452.
- 523 [15] F.P. O’Mara, The significance of livestock as a contributor to global greenhouse gas  
524 emissions today and in the near future, Anim. Feed Sci. Technol. 166–167 (2011) 7–15.  
525 doi:10.1016/j.anifeedsci.2011.04.074.
- 526 [16] O. Desrues, C. Fryganas, H.M. Ropiak, I. Mueller-Harvey, H.L. Enemark, S.M. Thamsborg,  
527 Impact of chemical structure of flavanol monomers and condensed tannins on *in vitro*  
528 anthelmintic activity against bovine nematodes., Parasitology. 143 (2016).
- 529 [17] M.T. Engström, M. Karonen, J.R. Ahern, N. Baert, B. Payré, H. Hoste, J.P. Salminen,  
530 Chemical Structures of Plant Hydrolyzable Tannins Reveal Their *in Vitro* Activity against  
531 Egg Hatching and Motility of *Haemonchus contortus* Nematodes, J. Agric. Food Chem. 64  
532 (2016) 840–851. doi:10.1021/acs.jafc.5b05691.
- 533 [18] M. Karonen, M. Oraviita, I. Mueller-Harvey, J.P. Salminen, R.J. Green, Binding of an  
534 Oligomeric Ellagitannin Series to Bovine Serum Albumin (BSA): Analysis by Isothermal  
535 Titration Calorimetry (ITC), J. Agric. Food Chem. 63 (2015) 10647–10654.  
536 doi:10.1021/acs.jafc.5b04843.
- 537 [19] N. Baert, W.F. Pellikaan, M. Karonen, J.-P. Salminen, A study of the structure-activity  
538 relationship of oligomeric ellagitannins on ruminal fermentation *in vitro*, J. Dairy Sci. 99

- 539 (2016) 8041–8052. doi:10.3168/jds.2016-11069.
- 540 [20] J. Quijada, C. Fryganas, H.M. Ropiak, A. Ramsay, I. Mueller-Harvey, H. Hoste,  
541 Anthelmintic Activities against *Haemonchus contortus* or *Trichostrongylus colubriformis*  
542 from Small Ruminants Are Influenced by Structural Features of Condensed Tannins, J.  
543 Agric. Food Chem. 63 (2015) 6346–6354. doi:10.1021/acs.jafc.5b00831.
- 544 [21] V. Spiegler, E. Liebau, A. Hensel, Medicinal plant extracts and plant-derived polyphenols  
545 with anthelmintic activity against intestinal nematodes, Nat. Prod. Rep. 34 (2017) 627–643.  
546 doi:10.1039/C6NP00126B.
- 547 [22] T.J. Bond, J.R. Lewis, A. Davis, A.P. Davis, Analysis and Purification of Catechin and Their  
548 Transformation Products, in Methods in Polyphenol Analysis, C. Santos-Buelga, G.  
549 Williamson (Eds.), (2003) pp. 229–265.
- 550 [23] T. Esatbeyoglu, V. Wray, P. Winterhalter, Isolation of dimeric, trimeric, tetrameric and  
551 pentameric procyanidins from unroasted cocoa beans (*Theobroma cacao* L.) using  
552 countercurrent chromatography, Food Chem. 179 (2015) 278–289.  
553 doi:10.1016/j.foodchem.2015.01.130.
- 554 [24] T. Esatbeyoglu, P. Winterhalter, Preparation of dimeric procyanidins B1, B2, B5, and B7  
555 from a polymeric procyanidin fraction of black chokeberry (*Aronia melanocarpa*), J. Agric.  
556 Food Chem. 58 (2010) 5147–5153. doi:10.1021/jf904354n.
- 557 [25] N. Köhler, V. Wray, P. Winterhalter, Preparative isolation of procyanidins from grape seed  
558 extracts by high-speed counter-current chromatography, J. Chromatogr. A. 1177 (2008) 114–  
559 125. doi:10.1016/j.chroma.2007.11.028.
- 560 [26] V. Pedan, N. Fischer, S. Rohn, Extraction of cocoa proanthocyanidins and their fractionation  
561 by sequential centrifugal partition chromatography and gel permeation chromatography,  
562 Anal. Bioanal. Chem. (2016) 5905–5914. doi:10.1007/s00216-016-9705-7.
- 563 [27] R.H. Brown, I. Mueller-harvey, W.E. Zeller, L. Reinhardt, E. Stringano, A. Gea, C. Drake,

- 564 H.M. Ropiak, C. Fryganas, A. Ramsay, E.E. Hardcastle, Facile Purification of Milligram to  
565 Gram Quantities of Condensed Tannins According to Mean Degree of Polymerization and  
566 Flavan-3-ol Subunit Composition, *J. Agric. Food Chem.* 65 (2017) 8072–8082.  
567 doi:10.1021/acs.jafc.7b03489.
- 568 [28] Z. Guadalupe, A. Soldevilla, M.P. Sáenz-Navajas, B. Ayestarán, Analysis of polymeric  
569 phenolics in red wines using different techniques combined with gel permeation  
570 chromatography fractionation, *J. Chromatogr. A.* 1112 (2006) 112–120.  
571 doi:10.1016/j.chroma.2005.11.100.
- 572 [29] N. Baert, M. Karonen, J.P. Salminen, Isolation, characterisation and quantification of the main  
573 oligomeric macrocyclic ellagitannins in *Epilobium angustifolium* by ultra-high performance  
574 chromatography with diode array detection and electrospray tandem mass spectrometry, *J.*  
575 *Chromatogr. A.* 1419 (2015) 26–36. doi:10.1016/j.chroma.2015.09.050.
- 576 [30] L. Montero, V. Sáez, D. von Baer, A. Cifuentes, M. Herrero, Profiling of *Vitis vinifera* L.  
577 canes (poly)phenolic compounds using comprehensive two-dimensional liquid  
578 chromatography, *J. Chromatogr. A.* 1536 (2018) 205–215.  
579 doi:10.1016/J.CHROMA.2017.06.013.
- 580 [31] A. Tuominen, M. Karonen, Variability between organs of proanthocyanidins in *Geranium*  
581 *sylvaticum* analyzed by off-line 2-dimensional HPLC-MS, *Phytochemistry.* 150 (2018) 106–  
582 117. doi:10.1016/J.PHYTOCHEM.2018.03.004.
- 583 [32] J. Hellström, J. Sinkkonen, M. Karonen, P. Mattila, Isolation and Structure Elucidation of  
584 Procyanidin Oligomers from Saskatoon Berries ( *Amelanchier alnifolia* ), *J. Agric. Food*  
585 *Chem.* 55 (2007) 157–164.
- 586 [33] I. McMurrough, D. Madigan, M.R. Smyth, Semipreparative Chromatographic Procedure for  
587 the Isolation of Dimeric and Trimeric Proanthocyanidins from Barley, *J. Agric. Food Chem.*  
588 44 (1996) 1731–1735. doi:10.1021/jf960139m.

- 589 [34] M.T. Engström, M. Päljjarvi, C. Fryganas, J.H. Grabber, I. Mueller-Harvey, J.P. Salminen,  
590 Rapid qualitative and quantitative analyses of proanthocyanidin oligomers and polymers by  
591 UPLC-MS/MS, *J. Agric. Food Chem.* 62 (2014) 3390–3399. doi:10.1021/jf500745y.
- 592 [35] J. Suvanto, L. Nohynek, T. Seppänen-Laakso, H. Rischer, J.P. Salminen, R. Puupponen-  
593 Pimiä, Variability in the production of tannins and other polyphenols in cell cultures of 12  
594 Nordic plant species, *Planta*. (2017) 1–15. doi:10.1007/s00425-017-2686-8.
- 595 [36] J.-P. Salminen, M. Karonen, Chemical ecology of tannins and other phenolics: we need a  
596 change in approach, *Funct. Ecol.* 25 (2011) 325–338. doi:10.1111/j.1365-  
597 2435.2010.01826.x.
- 598 [37] J.-P. Salminen, M. Karonen, K. Lempa, J. Liimatainen, J. Sinkkonen, M. Lukkarinen, K.  
599 Pihlaja, Characterisation of proanthocyanidin aglycones and glycosides from rose hips by  
600 high-performance liquid chromatography-mass spectrometry, and their rapid quantification  
601 together with Vitamin C, *J. Chromatogr. A*. 1077 (2005) 170–180.  
602 doi:10.1016/j.chroma.2005.04.073.
- 603 [38] L. Gu, M.A. Kelm, J.F. Hammerstone, Z. Zhang, G. Beecher, J. Holden, D. Haytowitz, R.L.  
604 Prior, Liquid chromatographic/electrospray ionization mass spectrometric studies of  
605 proanthocyanidins in foods, *J. Mass Spectrom.* 38 (2003) 1272–1280. doi:10.1002/jms.541.
- 606 [39] H.J. Li, M.L. Deinzer, Tandem mass spectrometry for sequencing proanthocyanidins, *Anal.*  
607 *Chem.* 79 (2007) 1739–1748. doi:10.1021/ac061823v.
- 608 [40] M. Karonen, J. Liimatainen, J. Sinkkonen, Birch inner bark procyanidins can be resolved  
609 with enhanced sensitivity by hydrophilic interaction HPLC-MS, *J. Sep. Sci.* 34 (2011) 3158–  
610 3165. doi:10.1002/jssc.201100569.
- 611 [41] A.B. Howell, J.D. Reed, C.G. Krueger, R. Winterbottom, D.G. Cunningham, M. Leahy, A-  
612 type cranberry proanthocyanidins and uropathogenic bacterial anti-adhesion activity,  
613 *Phytochemistry*. 66 (2005) 2281–2291. doi:10.1016/j.phytochem.2005.05.022.
- 614

615 **10 Tables**

616 Table 1. The plant species and tissues used in this study.

Plant Species			Sephadex LH-20 fractions 6	
Latin name	Common name	Plant tissue	<sup>a</sup> mDP	<sup>b</sup> PC/PD ratio
<i>Salix phylicifolia</i> L.	Tea-leaved willow	leaves	20	15/85
<i>Pinus sylvestris</i> L.	Scots pine	needles	18	24/76
<i>Aesculus hippocastanum</i> L.	Horse-chestnut	leaves	4	99/1
<i>Larix</i> sp	-	needles	12	62/38
<i>Trifolium repens</i> L.	White clover	flowers	18	2/98
<i>Trifolium medium</i> L.	Zigzag clover	flowers	9	99/1
<i>Ribes alpinum</i> L.	Alpine currant	leaves	19	3/967
<i>Lysimachia vulgaris</i> L.	Garden loosestrife	flowers	20	27/73
<i>Rhododendron schlippenbachii</i> Maxim.	The royal azalea	leaves	6	78/22
<i>Rhododendron dichroanthum</i> Diels.	-	leaves	5	79/21
<i>Lotus corniculatus</i> L.	Birdsfoot trefoil	green brownish pods	14	45/55

<sup>a</sup>Mean degree of polymerization (mDP) and <sup>b</sup>ratio of procyanidin and prodelphinidin subunits (PC/PD) measured by UPLC-MS/MS [32].

617

618 Table 2. Interpretations of the high-resolution mass spectrum of *Lythrum salicaria* semipreparative LC fraction 67. The numbering of the  
 619 oligomeric series refers to Figure 7.

Oligomer series	monoisotopic $m/z$ value of the most abundant oligomer	Charge state	Measured accurate mass (amu)	Mass error (ppm)	PA units in the most abundant oligomer		The range of monomer units per oligomer series	
					PC	PD	PC	PD
DP 2 & 4	584.1233	2	1170.2612	-2.49	3	1	4-0	0-4
	577.1338	1	578.1411	-2.32	2	0	0	2
DP 5	720.1572	2	1442.3289	-2.58	5	0	5-0	0-5
DP 3 & 6	865.1938	1	866.2011	-5.48	3	0	2-0	1-3
	864.1881	2	1730.3907	-3.06	6	0	5-0	1-6
DP 10	1002.5259	3	3010.5995	-3.12	2	8	9-2	1-8
DP 7	1008.2207	2	2018.4559	-1.71	7	0	7-1	0-6
DP 11	1098.5461	3	3298.6602	-3.67	3	8	10-1	1-10
DP 4,8,12	1201.2383	1	1202.2456	-6.97	1	3	4-0	0-4
	1160.2473	2	2322.5092	-3.64	7	1	8-1	0-7
	1205.2291	3	3618.7091	-4.53	2	10	10-0	2-12
DP 13	1301.2484	3	3906.7672	-5.56	3	10	10-2	3-11
DP 9	1352.2616	2	2706.5377	-4.74	2	7	8-1	1-8
DP 14	1402.6007	3	4210.8240	-5.51	3	11	9-1	5-13
DP 5,10,15	1505.2934	1	1506.3007	-7.68	1	4	5-0	0-5
	1496.2919	2	2994.5983	-5.22	3	7	9-2	1-8
	1493.2909	3	4482.8946	-4.70	5	10	11-2	4-13
DP 16	1594.6432	3	4786.9515	-4.69	5	11	8-2	8-14
DP 17	1701.3311	3	5107.0150	-2.38	4	13	9-2	8-14

622 Table 3. Interpretations of the high-resolution mass spectrum of *Lythrum salicaria* semipreparative LC fraction 91. The numbering of the  
 623 oligomeric series refers to Figure 8.

Oligomer series	Monoisotopic $m/z$ value of the most abundant oligomer	Charge state	Measured accurate mass (amu)	Mass error (ppm)	PA units in the most abundant oligomer		The range of monomer units per oligomer series	
					PC	PD	PC	PD
DP 5	720.1571	2	1442.32879	-2.64	5	0	4-5	1-0
DP 6	864.1881	2	1730.39073	-3.04	6	0	4-6	2-0
DP 10	959.8728	3	2882.64023	-3.23	10	0	9-10	1-0
DP 7	1008.2187	2	2018.45203	-3.64	7	0	5-7	2-0
DP 11	1055.8927	3	3170.69987	-4.12	11	0	9-11	3-0
DP 8 & 12	1152.2482	2	2306.51091	-5.14	8	0	8	0
	1151.9134	3	3458.76197	-4.15	12	0	10-12	2-0
DP 13	1247.9332	3	3746.82143	-4.88	13	0	11-13	2-0
DP 9&18	1296.2794	2	2594.57339	-4.92	9	0	8-9	1-0
	1295.7748	4	5187.12831	-5.47	18	0		
DP 14	1343.9534	3	4034.88200	-5.23	14	0	12-14	2-0
DP 19	1367.7890	4	5475.18507	-6.39	19	0	17-19	2-0
DP 5&10&15	1441.3134	1	1442.32067	-8.27	5	0	5	0
	1440.3091	2	2882.63283	-5.80	10	0	10	0
	1439.9738	3	4322.94311	-5.41	15	0	14-15	1-0
DP 21	1511.8209	4	6051.31251	-5.67	21	0	17-21	4-0
DP 16	1535.9923	3	4610.99864	-6.78	16	0	14-16	2-0
DP 11&22	1584.3389	2	3170.69239	-6.48	11	0	8-11	3-0
	1583.8351	4	6339.36931	-6.46	22	0	18-22	4-0
DP 17	1632.0130	3	4899.06086	-6.62	17	0	15-17	2-0
DP 23	1659.8492	4	6643.42591	-6.42	22	1	19-23	4-0
DP 18	1733.3691	3	5203.12901	-4.34	17	1	17-18	1-0
DP 25	1803.8793	4	7219.54639	-6.78	24	1	24-25	1
DP 19	1824.0519	3	5475.17765	-7.75	19	0	17-19	2-0

DP 20

1920.0731

3

5763.24122

-7.33

20

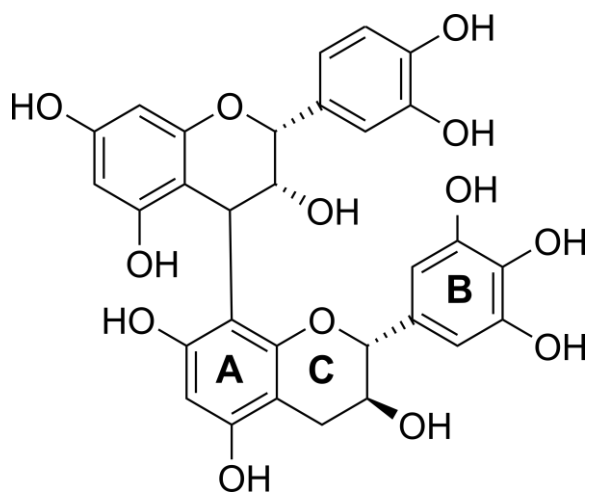
0

17-20

3-~~0~~24

---

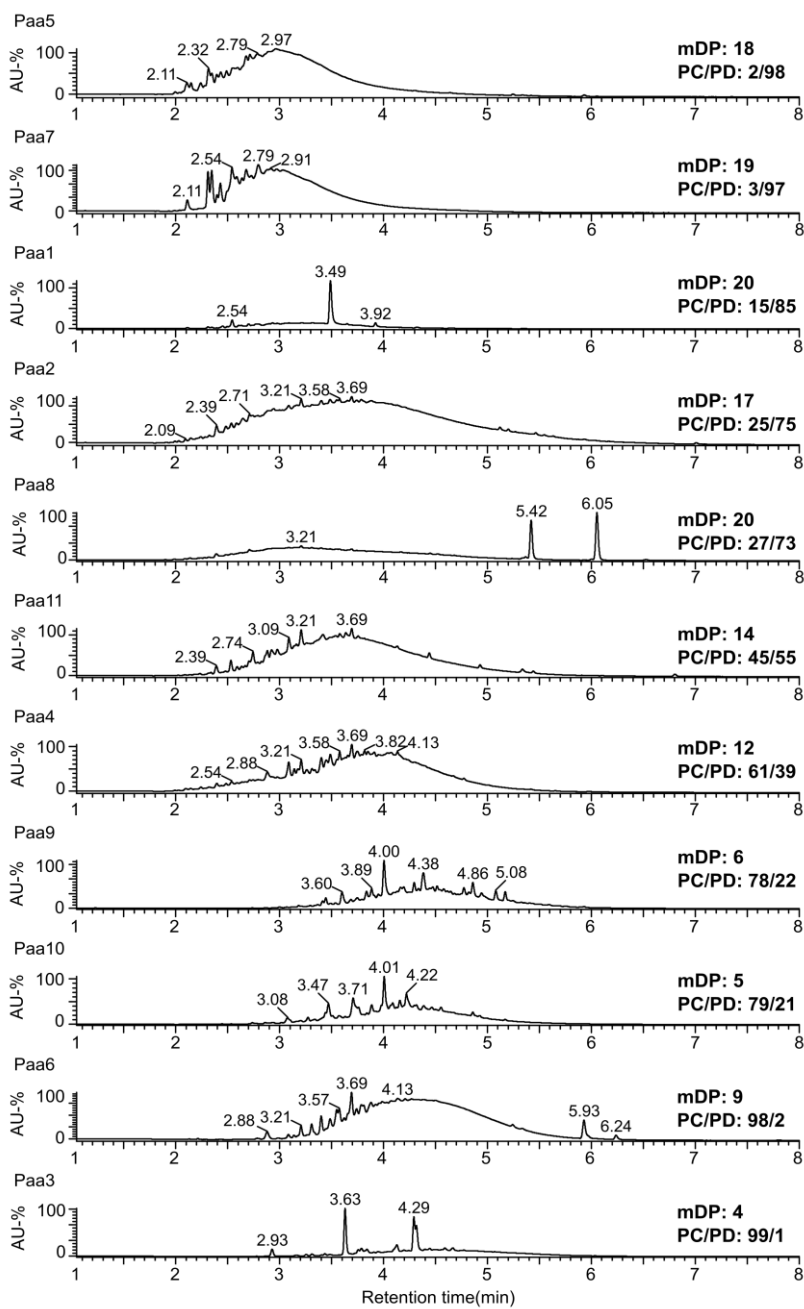
625 **11 Figures**



626

627 **Figure 1.** A dimeric proanthocyanidin consisting from the epicatechin extension unit and the  
628 gallocatechin terminal unit.

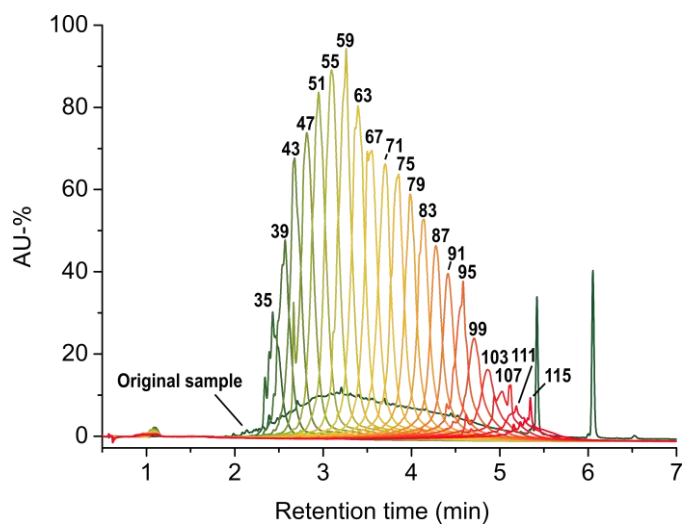
629



630

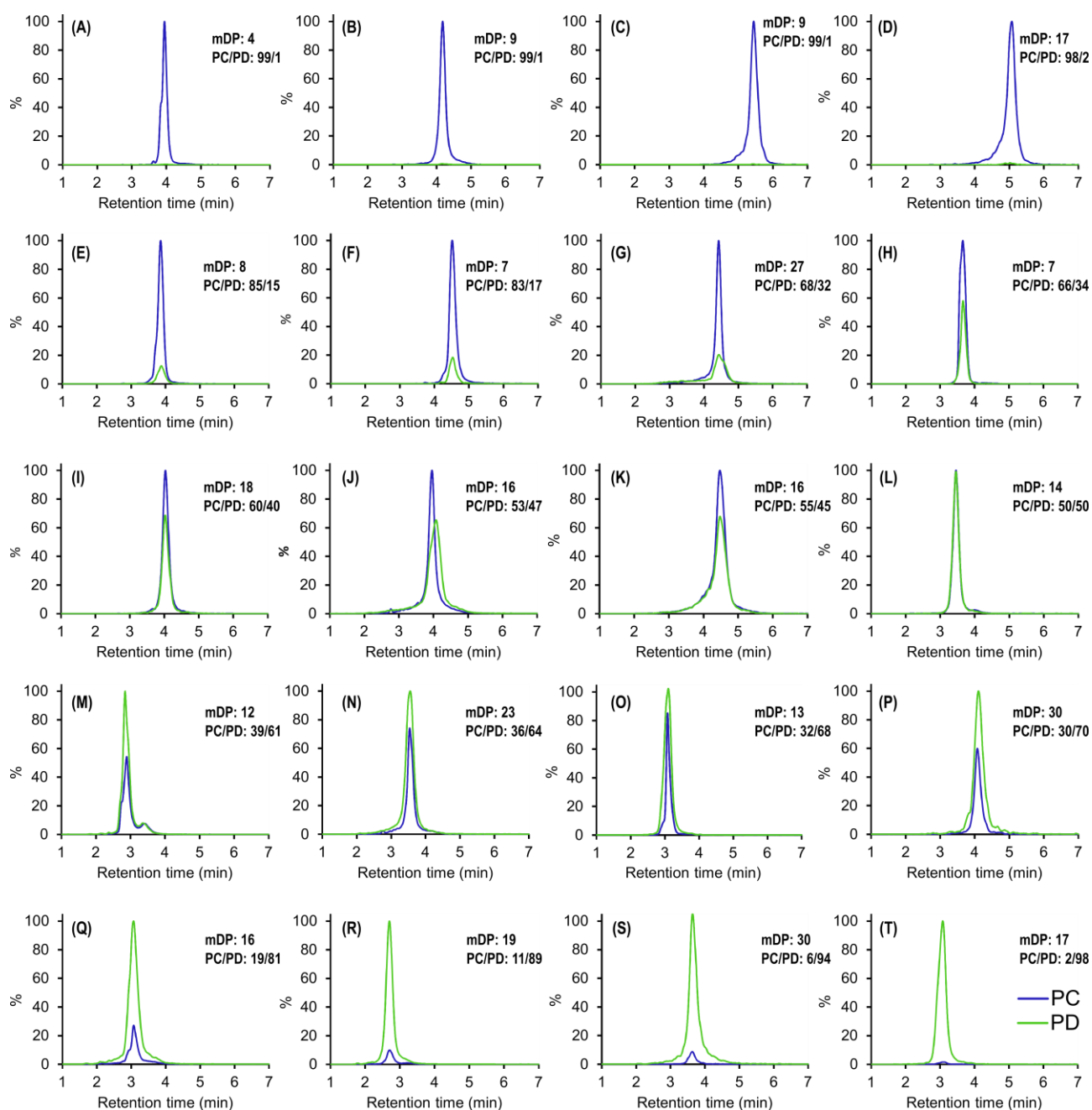
631 **Figure 2.** Semipreparative LC traces ( $\lambda = 280$  nm) of the proanthocyanidin rich 6<sup>th</sup> Sephadex LH 20

632 fractions.



633

634 **Figure 3.** UPLC–DAD chromatogram ( $\lambda = 280$  nm) of the 6<sup>th</sup> Sephadex LH-20 fraction of  
 635 *Lysimachia vulgaris* (original sample) and the further purified semipreparative fractions  
 636 ranging from fractions 35–115. Color gradient was used to distinguish fractions from each  
 637 other and the original sample is shown in dark green.



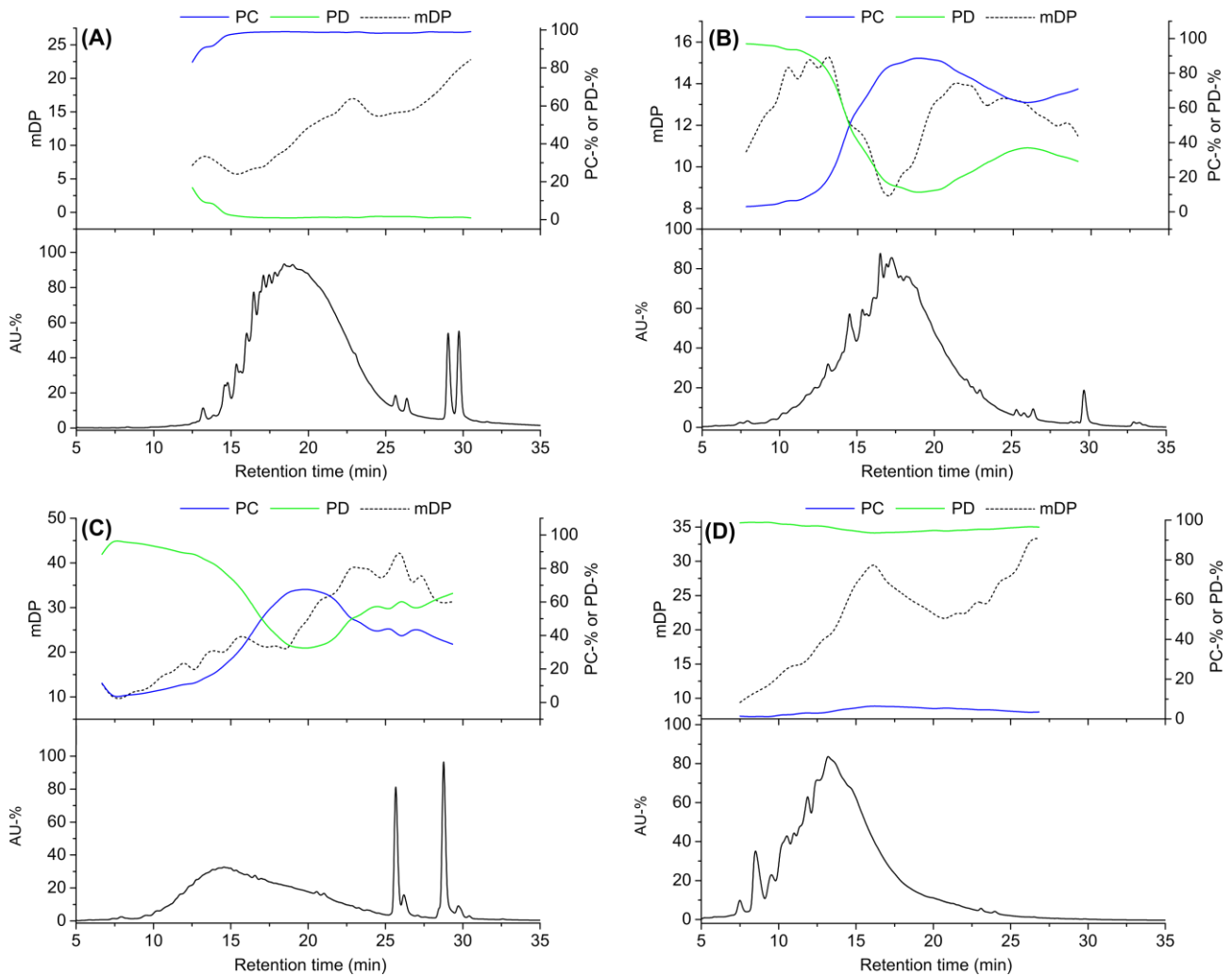
638

639 **Figure 4.** Combined UPLC–DAD–MS/MS single reaction monitoring traces of procyanidin (PC,  
 640 blue) and prodelphinidin (PD, green) units of semipreparative LC fractions (fr) of (A) *A.*  
 641 *hippocastanum* fr 76, (B) *T. medium* fr 82, (C) *A. hippocastanum* fr 116, (D) *T. medium* fr  
 642 106, (E) *Larix sp.* fr 74, (F) *R. dichroanthum* fr 92, (G) *L. vulgaris* fr 91, (H) *R.*  
 643 *schlippenbachii* fr 70, (I) *L. corniculatus* fr 80, (J) *L. coniculatus* fr 92, (K) *P. sylvestris* fr  
 644 78, (L) *L. corniculatus* fr 64, (M) *L. corniculatus* fr 48, (N) *L. vulgaris* fr 67, (O) *Larix sp.* fr

645

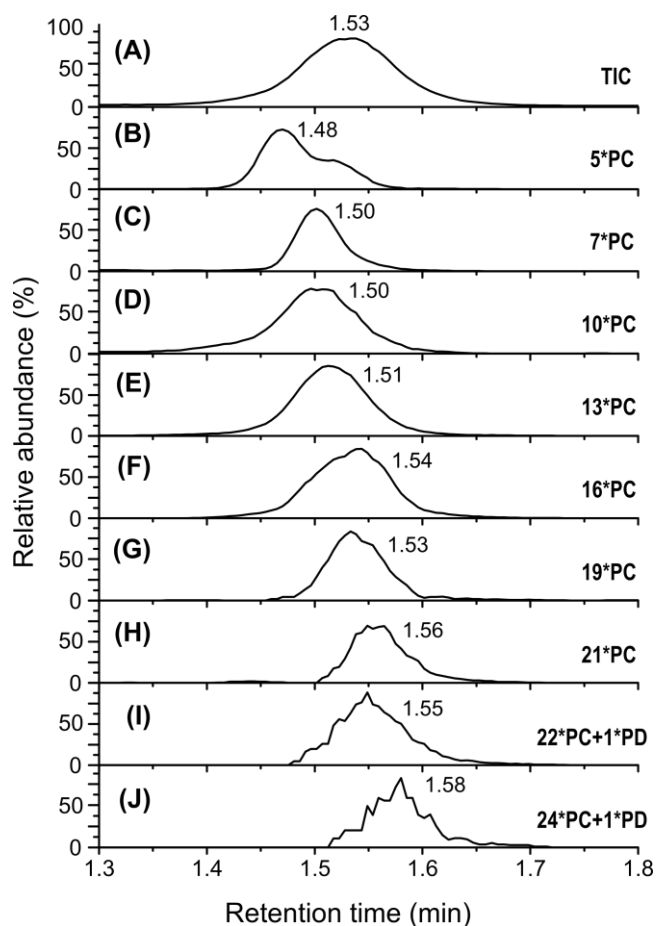
54, (P) *S. phyllicifolia* fr 80, (Q) *P. sylvestris* fr 54, (R) *L. vulgaris* fr 43, (S) *R. alpinum* fr 68

646

and (T) *T. repens* fr 54.

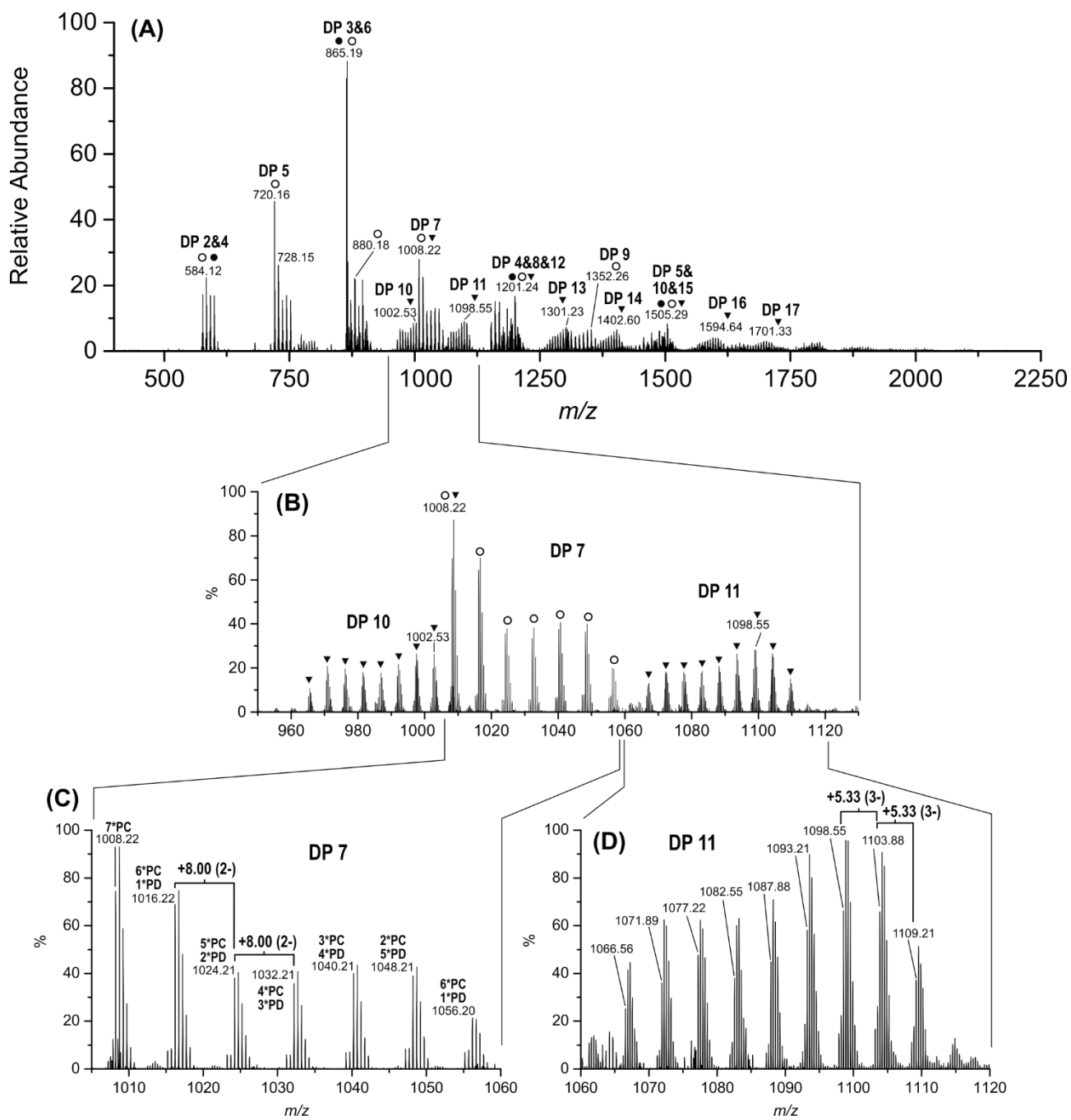
647

648 **Figure 5.** Semipreparative LC UV traces ( $\lambda = 280$  nm) are displayed in lower panels and the  
 649 distribution of the mean degree of polymerization (mDP), as well as procyanidin (PC) and  
 650 prodelfhinidin (PD) percentages are displayed in the upper panels. The samples shown are  
 651 Sep6 fractions of (A) *Trifolium medium*, (B) *Larix sp.*, (C) *Lysimachia vulgaris* and (D)  
 652 *Ribes alpinum*.



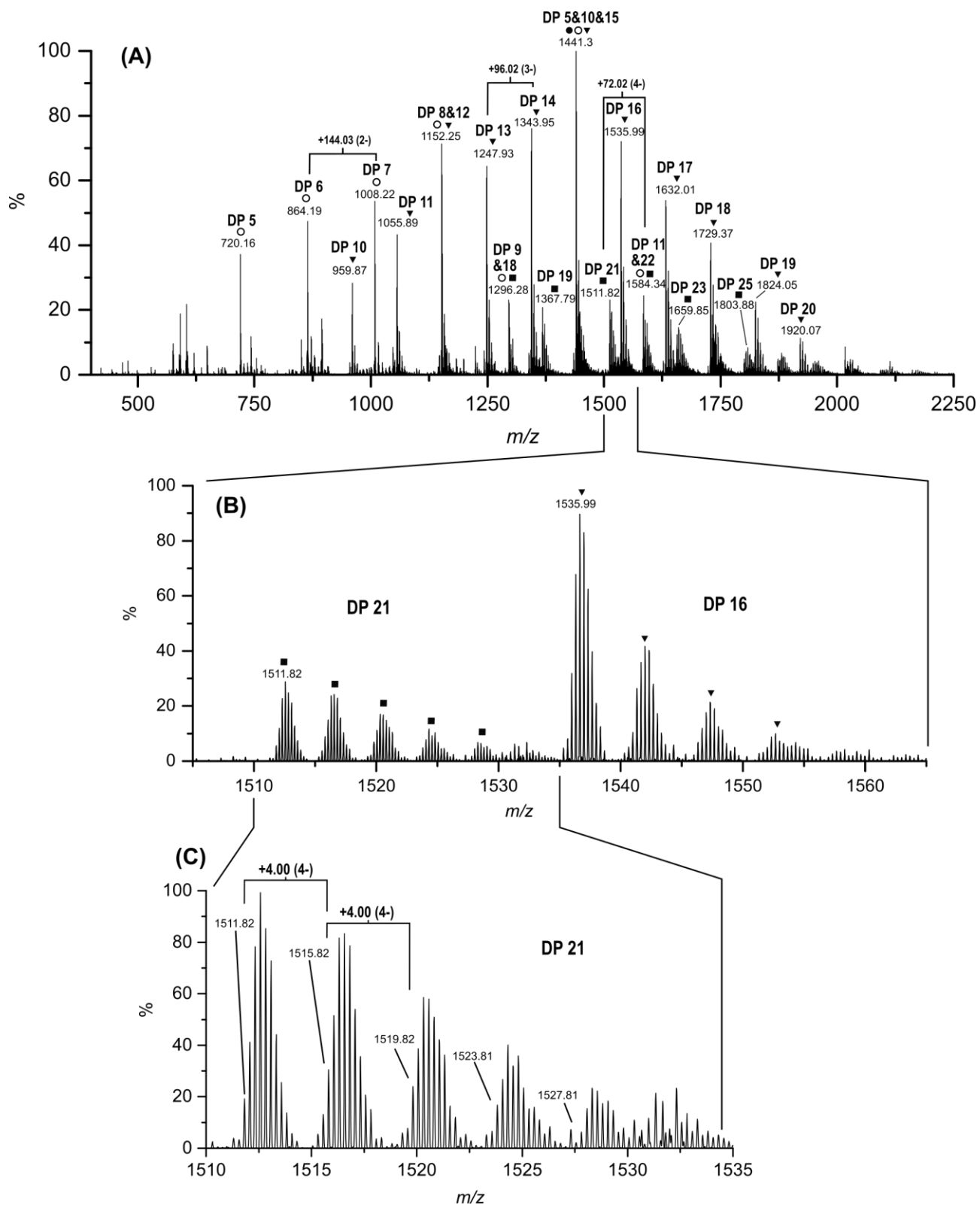
653

654 **Figure 6.** Total ion chromatogram (TIC) and extracted ion chromatograms (EICs) of *Lysimachia*  
 655 *vulgaris* semipreparative LC fraction 91 obtained by HRMS. The chromatograms are listed  
 656 as follows: (A) Total ion chromatogram (TIC), and EICs at (B)  $m/z$  720.13–720.19, (C)  $m/z$   
 657 1008.18–1008.27, (D)  $m/z$  959.83–959.92, (E)  $m/z$  1247.88–1247.99, (F)  $m/z$  1535.92–  
 658 1536.08, (G)  $m/z$  1823.98–1824.16, (H)  $m/z$  1511.75–1511.89, (I)  $m/z$  1659.78–1659.92, and  
 659 (J)  $m/z$  1803.80–1803.96. PC refers to procyanidin and PD to prodelphinidin unit, DP refers  
 660 to degree of polymerization.



661

662 **Figure 7.** High-resolution mass spectra of *Lysimachia vulgaris* semipreparative LC fraction 67 (A)  
 663 at  $m/z$  400–2250, (B) at  $m/z$  950–1125, (C) at  $m/z$  1005–1060, (D) at  $m/z$  1060–1120. The  
 664 symbols indicate the charge state of the ions as follows, (●) black dot  $[M-H]^-$ , (○) white dot  
 665  $[M-2H]^{2-}$ , (▼) inverted triangle  $[M-3H]^{3-}$ . DP refers to degree of polymerization. The  
 666 interpretations are listed in Table 2.



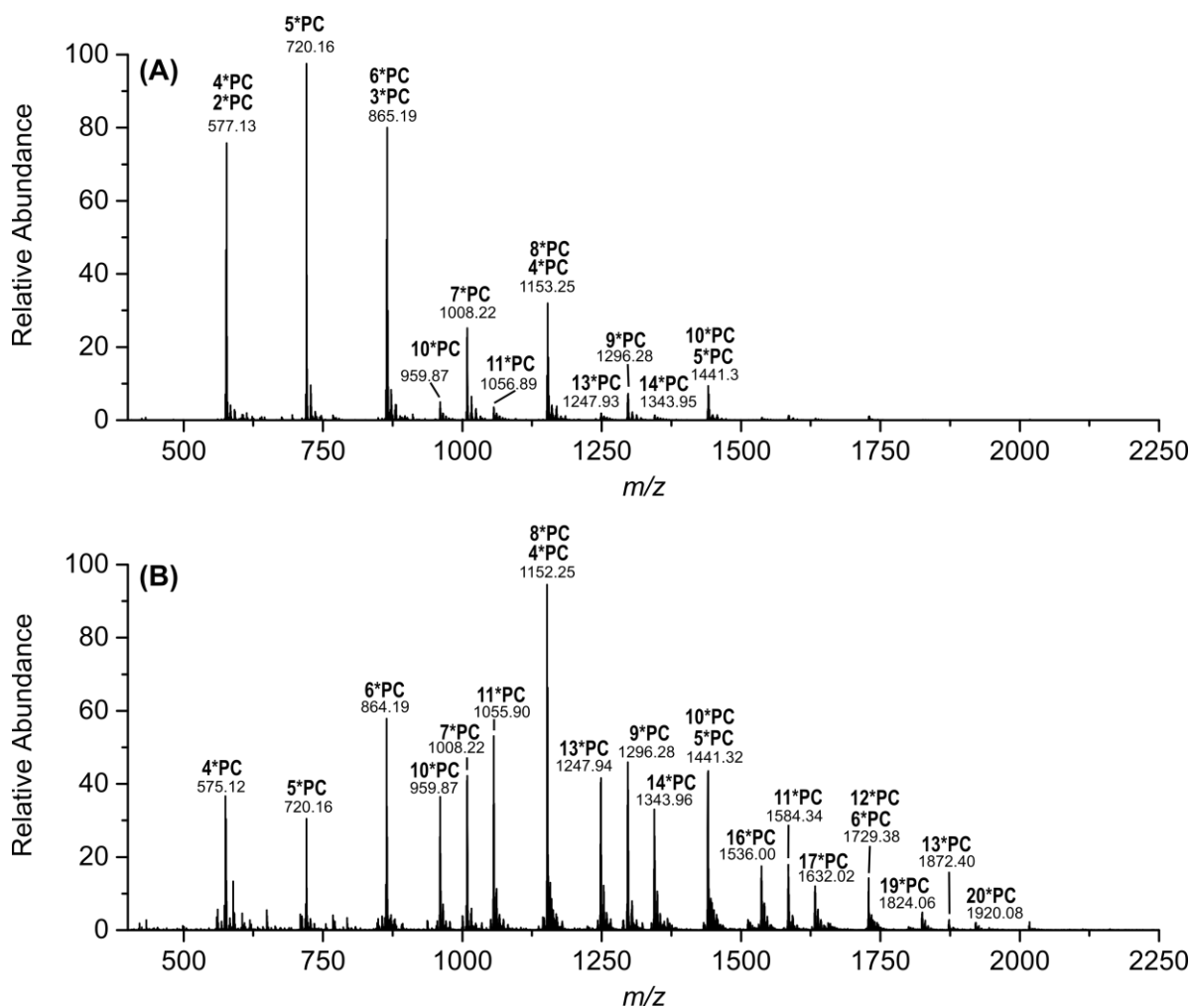
667

668 **Figure 8.** High-resolution mass spectra of *Lysimachia vulgaris* semipreparative LC fraction 91 (A)

669 at  $m/z$  400–2250, (B) at  $m/z$  1505–1565, (C) at  $m/z$  1510–1535. The symbols indicate the

670 charge state of the ions as follows ( $\circ$ ) white dot  $[M-2H]^{2-}$ , ( $\nabla$ ) inverted triangle  $[M-3H]^{3-}$ ,

671 (■) black square  $[M-4H]^{4-}$ . DP refers to degree of polymerization. The interpretations are  
672 listed in Table 3.



673  
674 **Figure 9.** HRMS spectra of the *Larix sp.* semipreparative LC fractions (A) 74 and (B) 94.  
675  
676